

Andrey Gritsun\*

# Low frequency variability and sensitivity of the Atlantic meridional overturning circulation in selected IPCC climate models

<https://doi.org/10.1515/rnam-2018-0029>

Received October 4, 2018; accepted October 22, 2018

**Abstract:** The structure of main modes of the decadal and multidecadal variability of the Atlantic meridional overturning circulation (AMOC) is analyzed for the climate models INM-CM5 (INM RAS), CCSM4 (NCAR), MPI-LR and MPI-MR (MPI). It is shown that oscillations with characteristic periods of 25–35 and 50–70 years are recognized in the models, and the corresponding spatial structures are variations of the intensity and position of the AMOC. Relations connecting changes of thermohaline circulation with external impacts on the system are constructed for the above models. The analysis of stability of calculations relative to the length of data series used for calculations is performed. The optimal impacts leading to the greatest response of the AMOC and influence functions causing its response along the leading modes of low-frequency variability are constructed. The optimal impacts have the form of density anomalies localized in the North Atlantic, and the structures of the corresponding responses are dominated by leading low-frequency modes of variability. The structure of optimal impacts varies greatly from model to model.

**Keywords:** Climate systems, variability, response, sensitivity, fluctuation–dissipation theorem, Atlantic meridional overturning circulation.

**MSC 2010:** 86-08, 82C05

---

**Dedicated to** the 80th anniversary of Prof. Valentin P. Dymnikov

Many important problems of modern geophysics require analysis of the reaction of the Earth climate system on external perturbations and search for optimal impacts causing the greatest possible response of the system. The studies of mechanisms of ocean circulation formation and, in particular, the nature of thermohaline overturning circulation maintenance in the Atlantic Ocean (hereinafter, AMOC) is not an exception. Since observational data are insufficient for full analysis of this phenomenon, the main way to study the problem are numerical simulations with numerical climate models. Unfortunately, the properties of the AMOC (in particular, spatial structure and the time spectrum of its variability) differ from model to model [12]. The mechanisms for maintaining the AMOC also vary from model to model and depend on both their spatial resolution and chosen parameterizations (vertical diffusion, vortex transport processes, description of subgrid processes in the Norwegian and Greenland seas, etc.) [5, 16]. In this regard, the problem of identification of models with respect to the sensitivity of the AMOC seems to be very important. We also note the widely discussed problem of interconnection between the AMOC and the Atlantic multidecadal oscillation manifesting differently in climatic models [18] with different physical mechanisms involved [4, 6].

The evaluation of the sensitivity of the AMOC involves the construction of perturbations with specific spatial structure causing the maximum possible (at a given magnitude of the impact) response of the system. There are two basic methods for obtaining such estimates, namely, the analysis of equations describing the dynamics of the climate system and the analysis of historical observation (or simulation) data archives. An example of the first approach is described in [2, 17], where numerical linearization of dynamics equations and subsequent analysis of the structure of singular vectors of the linear system were performed. The drawback

---

\*Corresponding author: Andrey Gritsun, Marchuk Institute of Numerical Mathematics of the RAS, Moscow 119333, Russia.

E-mail: [asgrit@mail.ru](mailto:asgrit@mail.ru)

of this approach (in addition to its complexity) is the sensitivity of results to the choice of the basic state against which the linearization is applied. The second approach (for example, [1]) is based on the search for events with significant anomalies of the AMOC in historical data archives (of simulations or observations) and analysis of the preceding circulation of the system. Since detailed data on the state of the AMOC in nature (especially its structure in the deep ocean) are available currently only for a small period of time, the second approach is used mainly for simulation data. Note that this method allows us to diagnose the states with abnormal dynamics and to a lesser extent serves for construction of optimal impacts on the system.

In this paper, in order to search for optimal impacts and influence functions, we use an alternative approach based on application of the fluctuation-dissipation relations [11, 13]. These relations being valid with high accuracy for a wide class of climate models associate the responses of a model to external influences with its statistical characteristics and allow us to evaluate approximately the sensitivity properties of a model. This approach is used to analyze the sensitivity of the AMOC for several models of leading climate centers (CCSM, MPI-ESM, and INM-CM) taking part in the climate model intercomparison projects lead by the Intergovernmental Panel on Climate Change (<http://www.ipcc.ch>).

## 1 Method of calculating the operator of system response to external impacts

A linear relation between external impacts on the system and the correspondent changes of its statistical characteristics is satisfied with a good accuracy for a wide class of systems, that is likely includes chaotic models of atmospheric and ocean dynamics. Strict justifications can be obtained, for example, within the framework of the theory of Fokker–Planck equation [13] of regular dynamics [11]. Let us consider some characteristic  $\varphi(X)$  of the system dependent on its state  $X(t)$ . The mean value of  $\varphi(X)$  can be obtained (under ergodicity condition) by averaging along a trajectory of the system or over the probability density of its states:

$$\bar{\varphi} \equiv \langle \varphi(X(t)) \rangle = \int \varphi(X) \rho(X) dX = \lim_{T \rightarrow \infty} \frac{1}{T} \int_0^T \varphi(X(t)) dt / T.$$

Here  $\rho(X)$  is the probability density (invariant measure) of states of the system and  $\langle \cdot \rangle$  denotes the averaging over the corresponding ensemble of states.

If an extremal action  $\delta f(t)$  affects the system, then  $\bar{\varphi}$  changes by a certain value  $\delta \bar{\varphi}(t)$  dependent on  $\delta f(t)$ . It was shown in the papers mentioned above that in the linear approximation (i.e., for small impacts) and under some additional assumptions the relation between  $\delta \bar{\varphi}(t)$  and  $\delta f(t)$  has the following form:

$$\delta \bar{\varphi}(t) = \int_0^t \left\langle \varphi(X(t)) \frac{\partial \rho(X(t))}{\partial X_k(t)} \Big|_{t=\tau} \right\rangle \delta f_k(\tau) d\tau.$$

This formula is a generalized fluctuation–dissipation relation, or FDR (see details in [13]). If  $\rho(X)$  is a normal distribution, then the relation takes the simpler form

$$\delta \bar{\varphi}(t) = \int_0^t \Sigma_{\varphi}(t - \tau) \Sigma(0)^{-1} \delta f(\tau) d\tau \quad (1.1)$$

where  $\Sigma_{\varphi}(t - \tau) = \langle \varphi(X(t)) [X'(\tau)]^T \rangle$  is the lagged covariance function with the lag  $t - \tau$  and  $\Sigma(0) = \langle X'(t) [X'(t)]^T \rangle$  is the covariance matrix of the system ( $X' = X(t) - \langle X \rangle$ ). This relation associates the response of the mean state of the value  $\bar{\varphi}$  at the time moment  $t$  to the impact  $\delta f$  acting in the time period  $[0, t]$  using statistical characteristics of the unperturbed system.

If the perturbation is acting in the time interval  $[0, \Delta]$  and does not vary spatial structure, and the response is averaging over the time interval  $[T_1, T_2]$ , then for the change  $\delta \varphi$  of the mean value we get

$$\delta\bar{\varphi} = \int_{T_1}^{T_2} \int_0^{\Delta} \Sigma_{\varphi}(t - \tau) \Sigma(0)^{-1} d\tau dt \delta f / (T_2 - T_1) \equiv M\delta f.$$

In this paper as  $\varphi$  we take the stream function  $\Psi_{AMOC}$  of the Atlantic meridional overturning circulation defined as follows:

$$\Psi_{AMOC}(z, y, t) = \int_z^{\Delta} \int_x V dx' dz'$$

where  $V$  is the longitudinal ( $y$ ) component of the flow velocity. The integration over the vertical coordinate appears here from the ocean bottom up to the level  $z$ , and the integration along the latitude (over  $x$ ) is performed from the Western to Eastern Atlantic boundaries. As the state vector  $X$  we take the ocean temperature (SST) and salinity (SSS) fields on the surface.

Thus, the expression for  $M$  is a matrix of dimension  $K \cdot 2L$ , where  $K$  and  $L$  are the dimensions of the field  $\Psi_{AMOC}$  and the fields SSS and SST, respectively. Therefore,  $\delta f$  is an impact on the system in the surface temperature and salinity fields. In its turn, in order to determine  $M$ , we have to calculate the covariation matrix  $\Sigma(0)$  of the two-component field (SST, SSS) and the lagged covariance function between  $\Psi_{AMOC}$  and the pair of fields (SST, SSS) and perform necessary summation. Note that we must invert the covariance matrix to calculate  $M$ , which leads to numerical errors and requires regularization of the algorithm. A detailed description of the algorithm for construction of the approximate response operator relative to the climatic model CCSM4 was presented in [10]. In contrast with [10], in this paper we use a simplified description of the phase space of climate models, instead of three-dimensional velocity, temperature, and salinity fields, the vector  $X$  includes only two-dimensional fields SST and SSS. This reduction is mainly due to the insufficient amount of available data. The inversion of the covariance matrix in (1.1) is performed in the space of 40 leading eigenvectors.

The FDR for climate models is usually checked by the direct numerical experiments with the models. For example, it was shown in [10] that the approach described here can be used with sufficient accuracy to construct leading singular vectors of the response operator  $M$  for the CCSM-4L model. In spite of the fact that in this paper we use a simplified approximation method for the response operator compared to [10], the leading eigenvectors of the obtained operator (see Figs. 3-B5 and 3-C5) are close to the results from [10] (see Figs. 2 and 3 in [10]). Thus, there are reasons to believe that for other considered models of similar complexity studied here the FDR gives a sufficiently reliable evaluation of leading singular vectors of the response operator.

By definition, the influence function  $g_j$ ,  $j = 1, \dots, 2L$ , for some state  $\alpha$  of the AMOC streamfunction is the result of summation of rows of the matrix  $M$  with the weights equal to the corresponding components  $\alpha_i$ , i.e.,

$$g_j = \sum_{i=1, K} \alpha_i M_{ij}, \quad j = 1, \dots, 2L \quad (1.2)$$

being in our case a vector of dimension  $2L$ . A significant value of the influence function at a point of the geographic grid means that the anomaly of the corresponding sign specified in it causes a positive response in the direction  $\alpha$ .

## 2 Models and data

In this paper we analyze several climate models included into the international project CMIP on comparison of climate models.

### 2.1 Climate models CCSM4 and CCSM4-L

Models of the CCSM family were developed at the National Center for Atmospheric Research of the USA. In this paper we use the results obtained by two versions of this model. The CCSM4 version [7] has the resolution of

1.25° in latitude and 0.9° in longitude with 26 vertical layers in the atmosphere. The ocean block of the model has the resolution of 1.1° in longitude, a variable resolution of 0.27–0.54° in latitude, and 60 vertical levels. Within the framework of the CMIP5 experiment with this model, the calculation of pre-industrial climate was performed for the period of 1100 years. The low spatial resolution model CCSM4-L citer14 has the horizontal resolution of 3.75° in the atmosphere and 3° in the ocean. Similar calculations for the period of 16000 years were performed for this model.

## 2.2 Climate models MPI-ESM-MR and MPI-ESM-LR

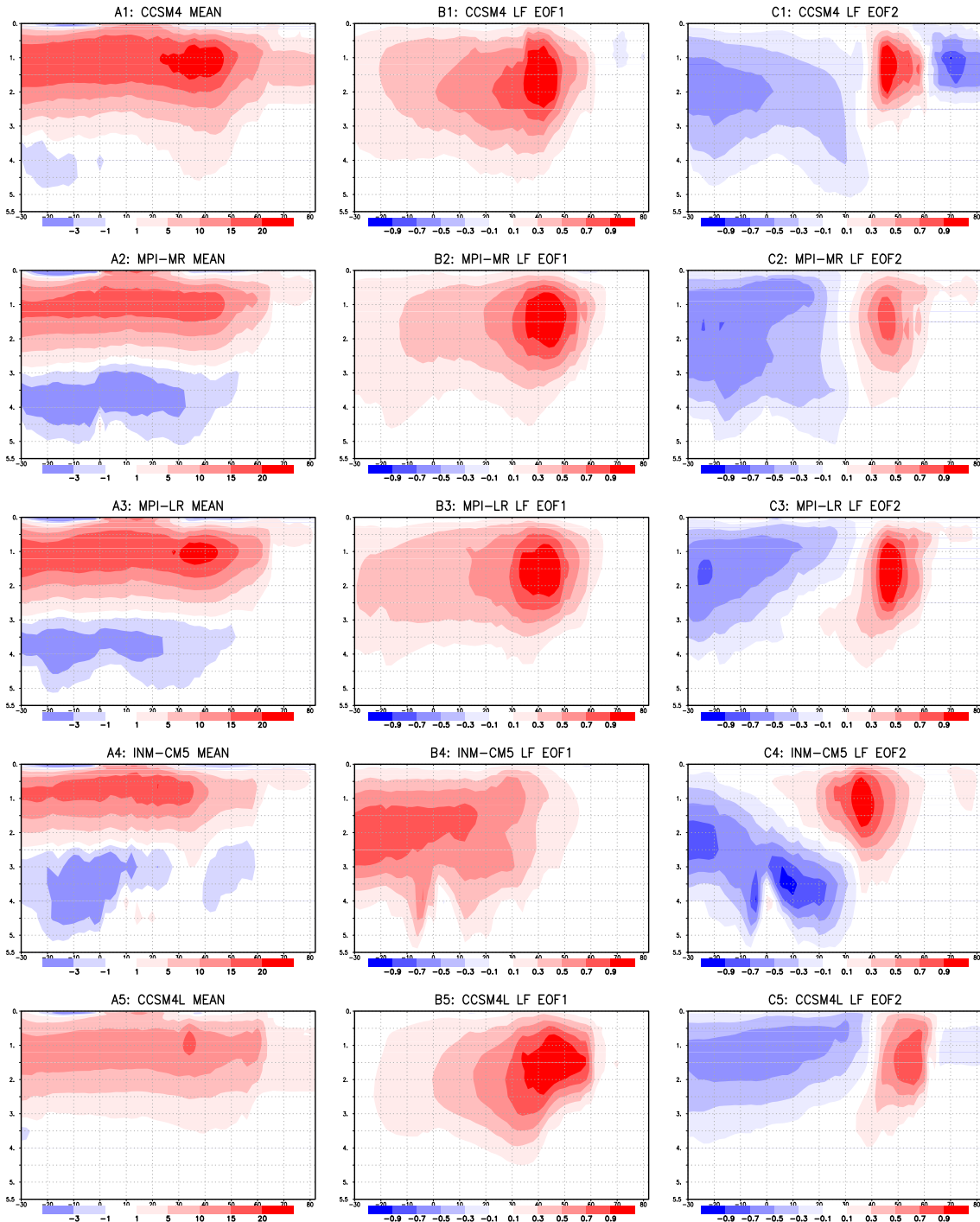
In this paper we analyze two versions of models of the family MPI-ESM [8] developed at the Max Planck Institute (Germany). The first version (MR) has 95 vertical layers and the horizontal resolution of 1.9° in the atmosphere, the horizontal resolution in the ocean is 0.4° with 40 vertical layers. The low-resolution model (LR version) uses 47 vertical layers in the atmosphere and the resolution of 1.5° in the ocean. Calculations of the pre-industrial climate were performed for the period of 1000 years with both these models within the CMIP5 experiment.

## 2.3 Climate model INM-CM5

In this paper we analyze the last model of the INM-CM family developed at the Institute of Numerical Mathematics of the RAS [15] being an upgrade of the INMCM4 model participating in the CMIP5 program. The model has the horizontal resolution in the atmosphere equal to 2 and 1.5 degrees in longitude and latitude, respectively, and 73 vertical levels. The horizontal resolution in the ocean is 0.5 and 0.25 degrees in longitude and latitude, the model has 40 vertical levels. Calculations of the pre-industrial climate were performed with this model for the period of 1200 years.

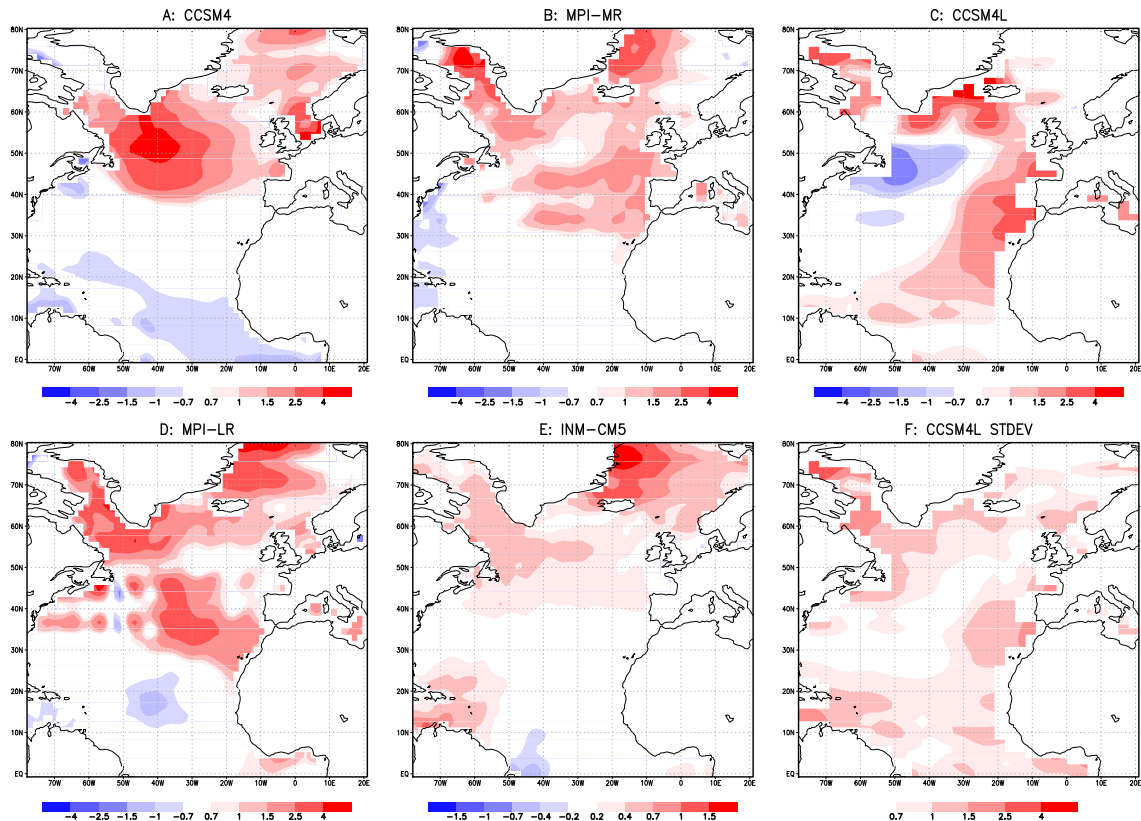
The mean monthly fields of the AMOC stream function as well as the temperature and salinity of the ocean surface were used to construct response operators and influence functions for all models. Since there is a trend in the model data (the model is drifting to the equilibrium climatic state), the 200-year moving average was removed from the data.

Figure 1 presents climatic characteristics of the Atlantic thermohaline circulation in the considered models. The left column (A1–A5) shows mean values of  $\Psi_{AMOC}$  for the models CCSM4 (A1), MPI-ESM-MR (A2), MPI-ESM-LR (A3), INM-CM5 (A4), and CCSM-4L (A5). The structure of circulation corresponds to the observed one in all the models. Note that INM-CM5 and CCSM-4L models have low values of the thermohaline transfer with the maximum of about 16 Sv ( $10^6 \text{ m}^3/\text{s}$ ). In addition, the basic cell of AMOC reaches only 40° N in the INM-CM5 model compared to 60° N in the other models. Another important characteristic of the circulation is empirical orthogonal functions (EOF) which are eigenvectors of the covariance matrix of the considered field, in this case,  $\Psi_{AMOC}$ . The leading vectors corresponding to the largest eigenvalues determine directions with the largest variability of this field. Figures 1B and 1C present low-frequency EOF fields of  $\Psi_{AMOC}$  (a filter removing all periods shorter than 10 years and longer than 100 years is applied to the field, then the covariance matrix is constructed, and after that the eigenvalue problem is solved for this matrix). In all models the first low-frequency EOF (see Fig. 1B) determines a considerable part of the variance of low-frequency oscillations (50%, 45%, 48%, 35%, and 35% in the models CCSM4, MPI-MR, MPI-LR, INM-CM5, and CCSM-4L, respectively) and is an oscillation of the AMOC intensity relative to the mean state. The oscillation spectrum in all models is dominated by periods of 50–70 and 25–35 years. The second leading low-frequency EOF in most models is the oscillation of the AMOC length (in the INM-CM5 model this is an oscillation of the AMOC depth), it corresponds to 15–20% of the total variance of the low-frequency variability depending on the model.



**Fig. 1:** Statistical characteristics of Atlantic meridional thermohaline circulation (left column (A1–A5) is for the mean state (Sverdrup), middle column (B1–B5) is for the leading low-frequency EOF (dimensionless), right column (C1–C5) is for the second low-frequency EOF (dimensionless) in climate models. Upper row (A1–C1) is for the CCSM4 model, 2nd row is for the MPI ESM MR model, 3rd row is for the MPI ESM LR model, 4th row is for the INM-CM5 model, 5th row is for the CCSM4 model of low resolution. The axis y is for depth in km, the axis x is for latitude.





**Fig. 2:** Influence functions (dimensionless) for excitation of the leading low-frequency EOF from Fig. 1 (B2) for the models CCSM4 (A), MPI-ESM-MR (B), CCSM4 of low resolution (C), MPI-ESM-LR (D), INM-CM5 (E). The field corresponding to the standard deviation in calculation of the Green function for case (C) is shown in (F).

### 3 Computational results

#### 3.1 Influence functions

In this paper we have constructed influence functions for leading modes of the low-frequency variability of  $\Psi_{AMOC}$ . To do this, for each model we constructed the response operator  $M$  by formula (1.1) and determine the corresponding influence functions by formula (1.2). The values  $T_1$  and  $T_2$  were taken equal to 1 and 5 years in (1.1) and  $\Delta$  was equal to 4 years. Therefore, the impact on the system lasts 4 years, the response is calculated for 4 years with delay equal to one year with respect to the beginning of the impact. In order to compare the models with each other (variability modes are different in different models), we performed the computations of influence functions for variability modes of the MPI-ESM-MR model (i.e.,  $\alpha$  in formula (1.2) is the field from Fig. 1-B2 or 1-C2). In order to simplify the visualization, the two-component influence function (for temperature and salinity) was recalculated into a single-component one (in terms of density) with the use of the simplest state equation.

The calculation results for the first mode (see Fig. 1-B2) are presented in Fig. 2 (A is the anomaly of density causing the response in the direction of this mode for the CCSM4 model, B is the same for the MPI-MR model, C is for the CCSM4-L model, D is for the MPI-LR model, E is for the INM-CM5 model). The analysis of Fig. 2 shows that the leading low-frequency mode in these models is caused by the anomalies of density (mainly in salinity) in the North Atlantic. Details of the influence function structure vary significantly from model to model. The closest models are MPI-LR and MPI-MR. The INM-CM5 model requires approximately three times stronger forcing to get a comparable in magnitude response along the structure of Fig. 1-B2 (the maximum

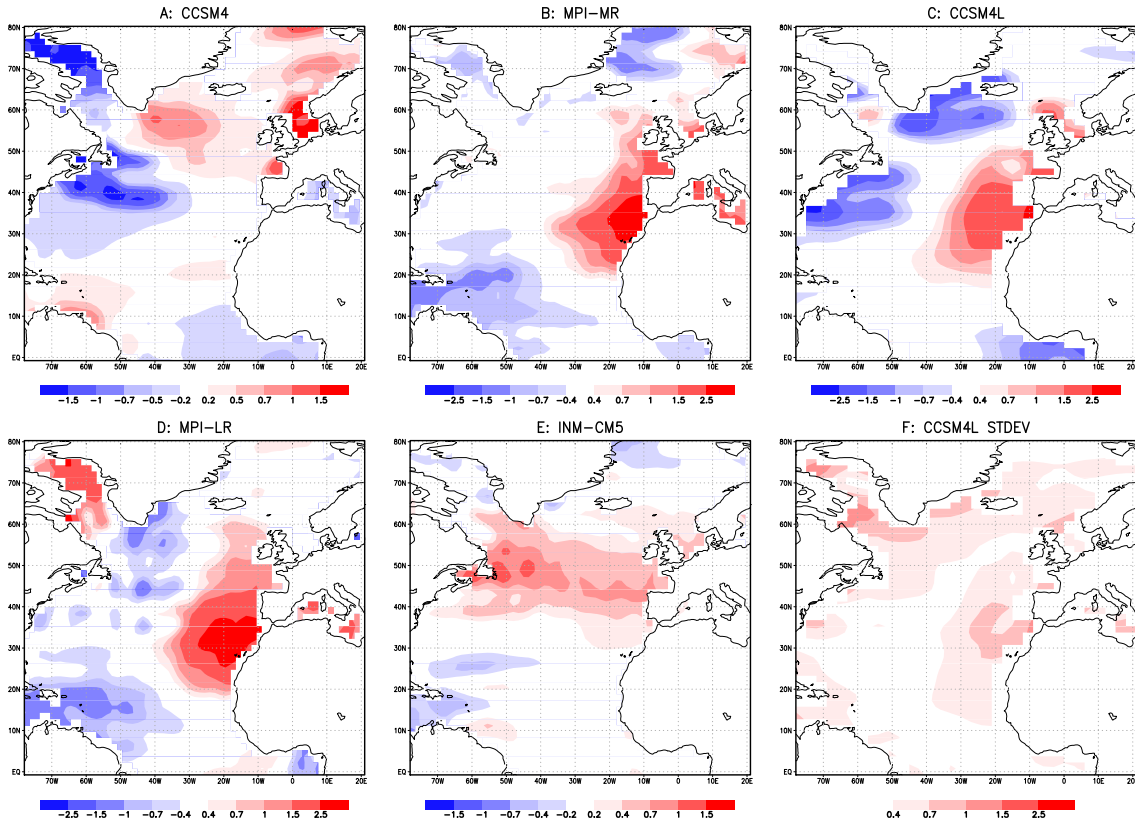


Fig. 3: The same as Fig. 2, but for the second leading EOF from Fig. 1-C2.

of the influence function in Fig. 2E is three times less than in other models). This seems to be a consequence of the fact that the structure of the first mode in the INM-CM5 model is not similar to the first mode in the MPI-MR model.

The sensitivity of the results to the amount of available data was estimated using the CCSM4-L model for which the series of available data is 16 times longer (16000 years). To do that, the influence function was calculated for each 1000-year period and then its variance was calculated from the obtained ensemble (16 implementations). The result of computation is shown in Fig. 2-F. We may conclude that the main structures of the influence functions calculated from the archive data with the length of 1000 years are significant.

The results of similar calculations for the second mode of the MPI-MR model (see Fig. 1-C2) are presented in Fig. 3. In this case the influence functions of the models MPI-MR (3B), MPI-LR (3D), and CCSM-4L (3C) are close. All these models have also close second low-frequency modes (see Figs. 1-C2, 1-C3, and 1-C5). The structures of influence functions for the models CCSM4 and INM-CM5 are essentially different. These models also require more strong impact to excite a response of the same amplitude than the models of the first group.

### 3.2 Optimal impacts and responses

Let us proceed to the analysis of leading singular vectors of the response operators  $M$  constructed by formula (1.1) for the models considered here. The first (A1–A5) and the third (C1–C5) columns in Fig. 3 contain the first and second leading left singular vectors (responses) of the mean value  $\Psi_{AMOC}$  on impacts in the density field on the surface. The corresponding impacts (right singular vectors) are shown in Fig. 3 in the second (B1–B5) and fourth (D1–D5) columns. The analysis of figures shows that the structure of leading responses is dominated by low-frequency modes of variability. This indicates that the ocean dynamics in the considered models

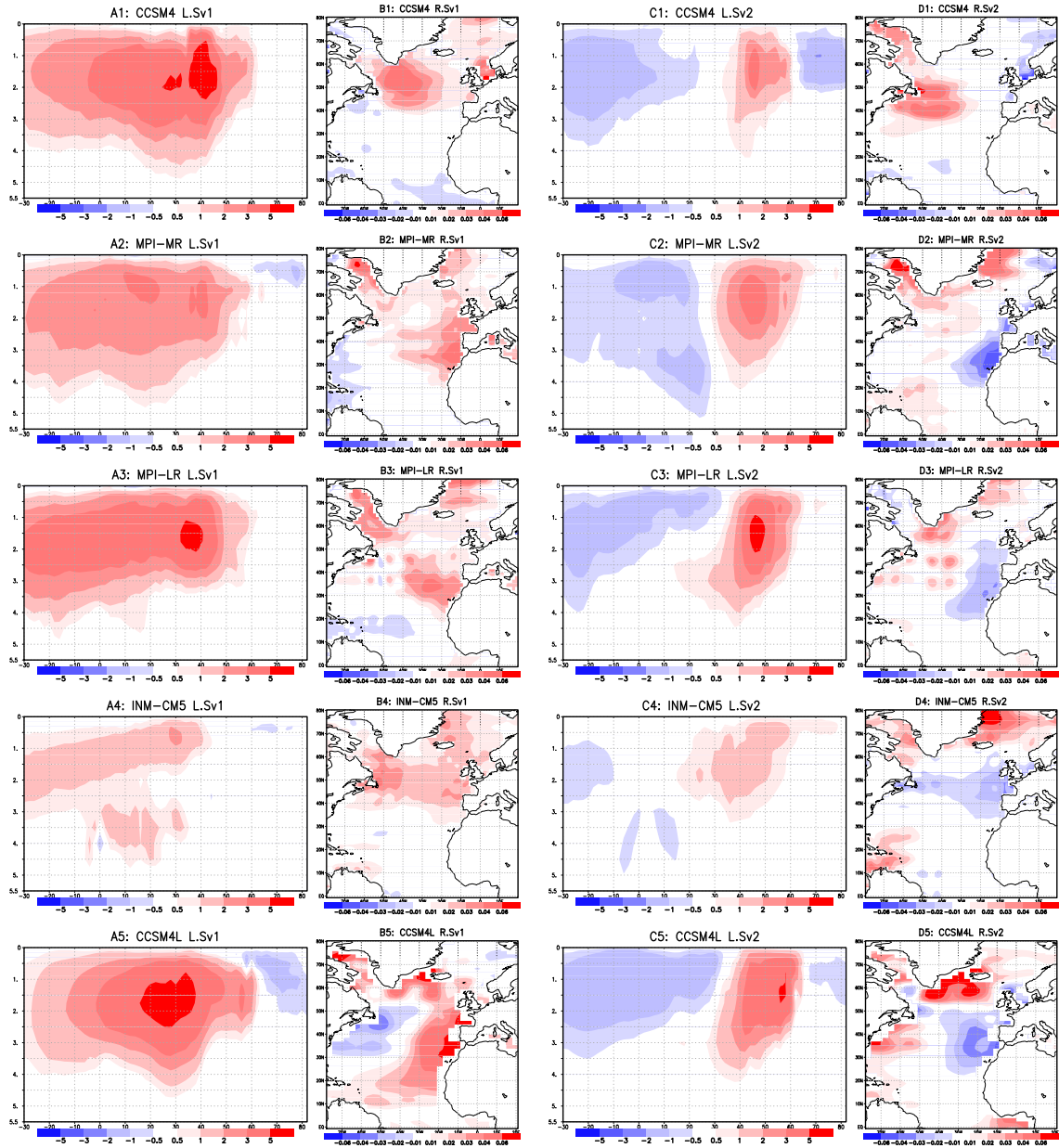


**Fig. 4:** First two pairs of leading singular vectors for the operator of response of the AMOC stream function on simultaneous impacts in the temperature and salinity fields in climate models (the first column is for the first left singular vector (response, dimensionless), the second column is for the first right singular vector (impact, dimensionless)), the third and fourth columns are for the same information for the second singular vector). The upper row (A1–D1) is for the CCSM4 model, 2nd row is for the MPI ESM MR model, 3rd row is for the MPI ESM LR model, 4th row is for the INM-CM5 model, 5th row is for the CCSM4 model of low resolution. The axis  $y$  is for depth in km, the axis  $x$  is for latitude. The normalization of impacts is the same everywhere.

can be described with a good accuracy by a linear dynamic-stochastic model [9]. The first mode is optimally excited in all models by a density anomaly located in the North Atlantic. The specific form of optimal impact in different models is different, but in close (in formulation) models (MPI-LR, MPI-MR) the optimal impacts are also close. Note that a structure similar to the optimal density anomaly for the CCSM4 model is also distinguished using regression analysis of the field  $\Psi_{AMOC}$  and temperature and salinity fields. For example, it was shown in [3] that exactly the same form of the density anomaly precedes the amplitude maximum of  $\Psi_{AMOC}$  in the CCSM4 model (in this case the delay interval is two years).



The second mode (oscillation of the AMOC position) is caused in most of the models by a dipole of density anomaly with a maximum near the Eastern Coast of Greenland and a minimum along the Atlantic Coast of Europe. The sensitivities (response amplitude) of most models are close, only the INM-CM5 model has approximately 2.5 times lower sensitivity.

In this paper we also consider the problem of optimal time for formation of a response to optimal impacts. Namely, at what value  $T_1$  in (1.1) will the amplitude of the model response be maximal (the values  $T_2 - T_1$  and  $\Delta$  are fixed by 4 years)? For models with higher spatial resolution in the ocean (CCSM4 and MPI-MR) this time is 3 years, for models with rough resolution (CCSM4-L and MPI-LR) the time of maximal response formation is 5 years. The INM-CM5 model is an exception, its horizontal resolution is  $0.5 \times 0.25$  degrees but the maximal response of the AMOC appears after the largest delay equal to 6 years relative to the initial moment of the anomaly forcing.

## 4 Conclusion

In this paper we present the analysis of the structure of the Atlantic meridional overturning circulation in the climate models INM-CM5 (INM RAS), CCSM4 (NCAR), MPI-LR and MPI-MR (MPI) and leading modes of its decadal and multidecadal variability. The structure of mean time circulation corresponds to the observed one in all the models. At the same time, the models INM-CM5 and CCSM-4L are characterized by lower values of thermohaline transfer with the maximum of about 16 Sv. In addition, in the model INM-CM5 the main cell of the AMOC reaches only  $40^\circ$  N compared to  $60^\circ$  N in other models.

Oscillations with typical periods of 25–35 and 50–70 years are distinguished in the models, which are variations of the intensity and position of the AMOC. In all the models, the leading mode determines a considerable part of the variance of low-frequency oscillations (50%, 45%, 48%, 35%, and 35% in the models CCSM4, MPI-MR, MPI-LR, INM-CM5, and CCSM-4L, respectively) and is an oscillation of the AMOC intensity relative to its mean state. The spectrum of oscillations in all the models is dominated by periods of 50–70 and 25–35 years. In most models the second leading low-frequency EOF is an oscillation of the AMOC length (in the INM-CM5 model it is an oscillation of the AMOC depth).

Further we analyze the sensitivity of thermohaline circulation in the Atlantic in the considered climate models. The analysis is based on an empirical approach, i.e., using the data of simulation of the pre-industrial climate, we construct approximate operators of the AMOC response to density anomalies with the use of fluctuation-dissipation relations. It is shown that the maximal response of the system relates to leading low-frequency modes of models and is caused by density anomalies (mainly in salinity) in the North Atlantic. The structure of optimal impacts changes significantly from model to model, however the similar in construction models MPI-LR and MPI-MR have also similar structure of optimal impacts. The sensitivity of most models to temperature and salinity anomalies on the surface is close. The exception is the INM-CM5 model whose response to an impact of similar magnitude is 2.5–3 times weaker.

**Funding:** The work was supported by the Russian Foundation for Basic Research (project 17–05–00628). The numerical experiment on calculating the pre-industrial climate for 1200 years with the INM-CM5 model and the analysis of its sensitivity were supported by the Russian Science Foundation (project 14–27–00126). Computational resources were provided by the JSCC RAS.

## References

- [1] L. C. Allison, E. Hawkins, and T. Woollings, An event-based approach to understanding decadal fluctuations in the Atlantic Meridional Overturning Circulation. *Clim. Dyn.* **44** (2013), No. 1–2, 163–190.
- [2] F. Cevillec, T. Huck, M. B. Jelloul, and N. Grimaet, Optimal surface salinity perturbations of the meridional overturning and heat transport in a global ocean general circulation model. *J. Phys. Oceanography* **38** (2008), No. 12, 2739–2754.

- [3] G. Danabasoglu, S. G. Yeager, Y.-O. Kwon, J. Tribbia, A. S. Phillips, J. W. Hurrell, Variability of the Atlantic meridional overturning circulation in CCSM4. *J. Climate* **25** (2012), 5153–5172.
- [4] T. Delworth, S. Manabe, and R. J. Stouffer, Interdecadal variations of the thermohaline circulation in a coupled atmosphere–ocean model. *J. Climate* **6** (1993), 1993–2011.
- [5] R. Farneti and G. K. Vallis, Mechanisms of interdecadal climate variability and the role of ocean–atmosphere coupling. *Climate Dyn.* **36** (2011), 289–308.
- [6] L. M. Frankcombe and H. A. Dijkstra, The role of Atlantic–Arctic exchange in North Atlantic multidecadal climate variability. *Geophys. Res. Lett.* **38** (2011), L16603/1–L16603/5.
- [7] P. R. Gent, G. Danabasoglu, L. J. Donner, M. M. Holland, E. C. Hunke, S. R. Jayne, D. M. Lawrence, R. B. Neale, P. J. Rasch, M. Vertenstein, P. H. Worley, Z.-L. Yang, and M. Zhang, The Community Climate System Model version 4. *J. Climate* **24** (2011), 4973–4991.
- [8] M. A. Giorgetta, J. Jungclaus, C. H. Reick, S. Legutke, J. Bader, M. Böttinger, V. Brovkin, T. Crueger, M. Esch, K. Fieg, K. Glushak, V. Gayler, H. Haak, H. Hollweg, T. Ilyina, S. Kinne, L. Kornblueh, D. Matei, T. Mauritsen, U. Mikolajewicz, W. Mueller, D. Notz, F. Pithan, T. Raddatz, S. Rast, R. Redler, E. Roeckner, H. Schmidt, R. Schnur, J. Segsneider, K. D. Six, M. Stockhause, C. Timmreck, J. Wegner, H. Widmann, K.-H. Wieners, M. Claussen, J. Marotzke, and B. Stevens, Climate and carbon cycle changes from 1850 to 2100 in MPI-ESM simulations for the Coupled Model Intercomparison Project phase 5. *J. Adv. Model. Earth Syst.* **5** (2013), 572–597.
- [9] A. S. Gritsun and V. P. Dymnikov, Barotropic atmosphere response to small external actions: Theory and numerical experiments. *Izv. Atmos. Oceanic Phys.* **35** (1999), No. 4, 511–525.
- [10] A. Gritsun, Numerical aspects of applying the fluctuation dissipation theorem to study climate system sensitivity to external forcings. *Russ. J. Numer. Anal. Math. Modelling* **31** (2016), No. 6, 339–354.
- [11] R. H. Kraichnan, Classical fluctuation–relaxation theorem. *Phys. Rev.* **113** (1959), 1181–1182.
- [12] Y.-O. Kwon and C. Frankignoul, Stochastically-driven multidecadal variability of the Atlantic meridional overturning circulation in CCSM3. *Clim. Dyn.* **38** (2012), 859–876.
- [13] H. Risken, *The Fokker-Planck Equation*, 2nd ed. Springer, Berlin, 1989.
- [14] C. A. Shields, D. A. Bailey, G. Danabasoglu, M. Jochum, J. T. Kiehl, S. Levis, and S. Park, The low-resolution CCSM4. *J. Climate* **25** (2012), 3993–4014.
- [15] E. M. Volodin, E. V. Mortikov, S. V. Kostykin, V. Ya. Galin, V. N. Lykossov, A. S. Gritsun, N. A. Diansky, A. V. Gusev, and N. G. Iakovlev, Simulation of the present day climate with the climate model INMCM5. *Clim. Dyn.* **49** (2017), 3715–3734.
- [16] S. G. Yeager and G. Danabasoglu, 2012: The sensitivity of Atlantic meridional overturning circulation variability to parameterized Nordic Sea overflows in CCSM4. *J. Climate* **25** (2012), 2077–2103.
- [17] L. Zanna, P. Heimbach, A. M. Moore, and E. Tziperman, 2011: Optimal excitation of interannual Atlantic meridional overturning circulation variability. *J. Climate* **24** (2011), 413–427.
- [18] L. Zhang and C. Wang, Multidecadal North Atlantic sea surface temperature and Atlantic meridional overturning circulation variability in CMIP5 historical simulations. *J. Geophys. Res. Oceans* **118** (2013), 5772–5791.